Native Ion Mobility Mass Spectrometry (IMMS) reveals that small organic acid fragments impart gasphase stability to carbonic anhydrase II

Native Ion Mobility Mass Spectrometry (IM-MS) reveals that small organic acid fragments impart gas-phase stability to carbonic anhydrase II

Clinton G. L. Veale[1], Maria Mateos-Jimenez[2], C. Logan Mackay[2], and David J. Clarke[2*]

1 School of Chemistry and Physics, Pietermaritzburg Campus
University of KwaZulu-Natal, Private Bag X01
Scottsville, 3209, South Africa
Email: VealeC@ukzn.ac.za

2 EaStCHEM School of Chemistry
University of Edinburgh, Joseph Black Building, David Brewster Road
Edinburgh, EH9 3FJ, UK.
E-mail: dave.clarke@ed.ac.uk

* Author for correspondence, email: dave.clarke@ed.ac.uk.

Short title: Fragment binding to Carbonic Anhydrase monitored by IM-MS.

ABSTRACT

Rationale

A key element of studies that utilise ion mobility mass spectrometry (IM-MS) under native electrospray conditions for the analysis of protein-ligand binding is the maintenance of a protein's native conformation during the removal of bulk solvent. Ruotolo and co-workers have demonstrated that the binding and subsequent dissociation of the anionic component of inorganic salts stabilises native protein conformations in the gas phase. In this study, we investigated the effect that organic acid fragments identified from a fragment-based drug discovery (FBDD) campaign might have on the gas-phase stability of carbonic anhydrase II (CA II).

Methods

Here we utilise native IM-MS to monitor changes in the conformation of CA II in the absence and presence of four acidic fragments. By performing a series of collisional induced unfolding (CIU) experiments we determine the effect of fragment binding on gas phase stability of CA II.

Results

Binding and dissociation of acidic fragments results in increased gas phase stability of CA II. Collision induced unfolding experiments revealed that the native-like compact gas phase conformation of the protein is stable with higher degree of pre-activation when bound to a series of acidic fragments. Importantly, even though acetate was present in high concentrations, the stabilising effect was not observed without the addition of the acidic fragments.

Conclusions

Binding and subsequent dissociation of acidic fragments from CA II significantly delayed CIU in a manner which is likely analogous to inorganic anions. Furthermore, we saw a slightly altered stabilising effect between the different fragments investigated in this study. This suggests that the prevention of CIU by organic acids, may be tuneable to specific properties of a bound ligand. These observations may open avenues to exploit IM-MS as a screening platform in FBDD.

1. Introduction

The ability to generate gas-phase ions of bio-macromolecules from pH controlled solutions has made it possible to utilise mass spectrometry (MS) to analyse complex biological systems under simulated physiological conditions.[1,2] This strategy, termed native mass spectrometry, has now become a common method for the direct monitoring of protein-ligand interactions,[3–5] and provides a comparatively fast and sensitive method of detecting relatively weak non-covalent interactions between picogram quantities of unlabelled proteins and ligands.[6–8] In particular, over the last decade native MS has shown great promise for the biophysical characterisation of candidate small molecule therapeutics and their binding to protein-targets in drug discovery programmes.[8]

More recently, ion-mobility (IM) has emerged as a complimentary technique in native MS studies, where measurements of a protein ions arrival time distribution (drift time), and collisional cross sections can assist in resolving questions related to biomolecule topology, conformational dynamics and ligand induced conformational changes.[9] Unsurprisingly, applications for assessing protein-ligand interactions using IM-MS are becoming increasingly common.[10–15] Especially useful is the ability to use IM to observe the gas phase unfolding of protein ions. Through the stepwise increase of acceleration potentials within the IM-MS instrument, the kinetic energy of protein ions can be sequentially increased by collisional heating prior to IM measurement. This vibrational activation results in gas phase unfolding of the protein which can be monitored by subsequent increase in drift time in the IM measurements.[16] Ruotolo and co-corkers have demonstrated that this collision induced unfolding (CIU) profile can be influenced by the presence of bound cations and anions[17–19]; which resulting in an increased lifetime of a compact protein species at elevated activation voltages. Furthermore, they demonstrated that anion induced protein stabilisation correlated with binding affinity with the protein.[18] Bound anions have been proposed to enhance protein stability due to dissociative cooling which removes rotational and vibrational energy from the gas phase protein.[20]

Based on the observation that inhibition of CIU through anion binding is related to protein affinity, we were curious as to whether this affect may also occur with organic molecules such as those encountered in fragment-based drug discovery (FBDD) campaigns. Typically, FBDD workflows utilise sensitive biophysical techniques to identify organic fragments, as a starting point for hit optimisation.[21] While this method has the advantage of increasing the efficiency by which relevant chemical space is explored, the typically lower binding affinity associated with fragments results in binding events which are easier to disrupt.[22] Native MS and IM-MS are both promising tools for screening protein-fragment binding in FBDD campaigns,[23,24] as potentially useful information may be extracted from both the native MS observations and the effect fragment binding has on protein stability determined by IM-based CIU experiments. Therefore, understanding how fragment-binding influences protein gas-phase stability is important if we are to fully leverage biological information from this biophysical technique.

In a recent study, Poulsen and co-workers[25] demonstrated that 3-phenoxy benzoic acid (**1,** Figure 1) bound to the active site zinc of carbonic anhydrase II (CA II), and this interaction was observable by native MS (Figure 2). To this end we were interested in observing the effect that this acid might have on gas phase protein stability of the CA II. In addition, experiments were conducted on four related fragments (**2 – 5**). 4-Phenoxy benzoic acid (**2**) and 2-phenoxy benzoic acid (**3**) were not reported as CA II binders, while the related 3-benzyloxy-phenylacetic acid (**4**), was reported as an CA II binder by Poulsen and coworkers.[25] Finally the methyl ester of compound **2** (**5**) was utilised as a non-acidic control. Interestingly, there is evidence for multiple binding sites for acidic molecules in CA II. Through a X-ray co-crystallisation study, Martin and Cohen showed that salicylic acid analogues **6** and **7** occupy both the zinc active site as well as an alternative binding site located roughly 14 Å away.[26] D'Ambrosio et al. further elucidated that increasing the steric bulk of the *ortho*-substituent such as with compound **8** resulted in preferential binding to the alternate region, over the catalytic site, due to steric clashes with catalytic site residues.[27] Importantly, **8** maintained CA II inhibitory activity, rendering it an allosteric inhibitor.[27] Poulsen and co-workers reported the binding of **9** through native MS, but did not obtain X-ray co-crystal to elucidate the binding site.[25] Therefore, it is possible that compound **3** may occupy the allosteric site rather that the catalytic site.

For the purposes of this study, we opted to screen at high fragment concentrations- mimicking conditions routinely used in early FBDD screening campaigns, where fragment dissociation constants are typically in the high μM range. An additional benefit of selecting CA II for this study, is that the zinc containing catalytic site binds to acetate anions.[28] Acetate is present in high concentrations in native MS, and is recognised as a moderately stabilising kosmotrope,[17] which could be exploited as a weakly binding internal control acid.

2. Experimental

2.1 Chemicals and Materials.

Carbonic anhydrase II and fragments **1-5** were all purchased from Sigma-Aldrich (St Louis, MO,USA). LC-MS grade DMSO and LC-MS grade ammonium acetate (NH_4OAc) were used in all studies and were purchased from Sigma-Aldrich (St Louis, MO,USA).

2.2 Sample preparation.

CA II is a highly conserved protein family and enzymes share similar structural folds and active site geometries.[29] For this study, samples of bovine carbonic anhydrase II (CA II) were dissolved in 10 mM NH_4OAc to a final concentration of 10 μM. (referred to here as apo CA II). For experiments involving fragments **1 – 3**; fragments were dissolved in 10 mM NH_4OAc buffer. For experiments involving fragments **4** and **5**, fragments were dissolved in LC-MS grade DMSO and solutions made up with 10 mM NH_4OAc buffer. Aliquots of the respective solutions of fragments **4** and **5** were added to a buffered solution of CA II in 10 mM NH_4OAc to a final concentration of 0.3% DMSO. Fragments were separately incubated with CA II to a final concentration of either 10, 50, 100, or 330 μM fragment and 10 μM CA II. For experiments involving KCl; KCl was dissolved in 10 mM NH_4OAc and added to a buffered solution of CA II to a final concentration of 60 μM KCl and 10 μM CA II.

2.3 Ion Mobility-Mass Spectrometry Analysis.

Mass spectra and ion mobility data were obtained on a Synapt-G2 Q-ToF mass spectrometer equipped with travelling wave ion mobility (TWIMS). Nano-ESI was performed using a Nanomate (Advion Bio-science) running in the positive ion infusion mode with an applied nanoelectrospray voltage of 1.54 V. For all experiments, the cone voltage, extract voltage and trap voltage were set at 20 V, 2V and 5 V respectively. To enhance the transmission of native protein ions the source temperature was lowered to 50 ^{o}C and the backing pressure was adjusted to 4.0 mbar resulting in a source pressure of 9.8e-4 mbar. For IM-MS measurements, the IMS wave height and IMS velocity were set at 22 V and 300 V respectively; IM-MS spectra were recorded for 5 minutes under each set of conditions. Collision induced unfolding (CIU) data was collected by increasing the trap voltage in increments of between 2 – 5 V up to a maximum of 80 V. Data processing to produce CIU plots was performed using CIU suite (University of Michigan).[16] For the protein-fragment complexes, the drift time data for all stoichiometric complexes within the same charge state were combined.

3. Results and Discussion

3.1 Native MS of fragment binding to Carbonic Anhydrase

Native state mass spectra were obtained for apo CA II as well as in the presence of high concentration (330 μM) of fragments **1 – 5**, typical for FBDD screens (Figure 2). In addition, mass spectra were recorded with protein:fragment ratios of 1:1, 1:5 and 1:10 in order to gauge protein-fragment affinity (Supporting Information, Figure S1). While the 10+ charge state was the dominant charge state for the mass spectra obtained for apo CA II as well as in the presence of fragments **1 – 3**, the inclusion of DMSO for the screening of fragments **4** and **5**, resulted in a resulted in a shift of the charge state distribution to a lower charge state resulting in the 9+ charge state being dominant, a phenomenon observed previously (Supporting Information, Figure S2A).[30] The native mass spectrum of apo CA II (Figure 2A) displayed a charge state distribution containing two charge states (9+ and 10+; Figure S2A). The 9+ charge state displayed a peak at *m/z* of 3233.2 which corresponded to a zinc bound CA II ion (i.e. $[M+Zn+7H]^{9+}$); in addition to a second peak at *m/z* 3239.8 which corresponds to the acetate bound species ($[M+Zn+CH_3COOH+7H]^{9+}$). Similarly, in the mass spectra obtained for CA II incubated with fragment **1** (Figure 2B), a portion of apo CA II with and without acetate adducts could be observed. In addition, a mass increase consistent with fragment binding was observed. Interestingly, the peak corresponding to the CA•**1** binding complex (*m/z* of 3257.0, $[M•\mathbf{1}+Zn+7H]^{9+}$, orange diamond) did not feature a major acetate binding adduct, suggesting that fragment **1** displaced acetate upon binding within the catalytic active site of CA II. X-ray co-crystal data has previously confirmed that compound **1** binds at this site of the CA II.[25] A similar trend was observed for fragment **2** (Figure 2C), with the fragment displacing acetate upon binding. This observation again suggests that binding of fragment **2** also occurs close to the active site of CA II, indicating a degree of specificity in the binding mode. The large excess of fragment in these experiments, chosen to mimic typical FBDD screening conditions, also leads to some presumably non-specific association of fragments to the protein with fragments

1 and **2** – indicated by the presence of a species 1:2 stoichiometric complex with lower ion abundance. In contrast, binding of fragments **3** to CA II did not result in displacement of the acetate anion, and the $[M•\mathbf{3}+Zn+CH_3COOH+7H]^{9+}$ is clearly observed (Fig 2D, orange asterisk), supporting the notion that this fragment occupies the allosteric binding site.[27] In addition, the binding stoichiometry observed with this fragment was more diverse, with **3** displaying stoichiometry between 1:1 and 1:4 (CA•fragment). These observations point to the binding of fragment **3** being more non-specific in nature and is perhaps mediated via ionic interaction on the surface of the protein and is not predominantly binding site occupation. In a similar manner fragment **4** also displayed a range of binding stoichiometry (1:1 to 1:7) with CA. However, there was evidence of acetate displacement upon binding and it is interesting to note that X-ray co-crystallography has shown that acid **4** binds to the CA II catalytic site.[25] Taken together, these finding suggest that both active site binding (displacing the acetate ion) and non-specific surface binding occur upon addition of **4** to CA under the conditions used. In contrast to all four free acid ligands, no binding was observed for methyl ester **5,** highlighting the importance of the acidic functionality for protein-ligand binding.

3.2 Ion Mobility and Collision induced unfolding (CIU) analysis of CA:fragment complexes.

Having established that acids **1 – 4** bind to CA II as well as confirming the importance of the free organic acid for this interaction, we subsequently monitored changes in the native mass spectrum and ion mobility drift time of the CA II ion as a function of collisional activation. During this CIU analysis, all experimental conditions were kept identical with the exception of trap voltage, which was increased stepwise up to 80 V. Initially we confirmed that the addition of 0.3% DMSO in the electrospray solution had no effect on the observed arrival time distributions of CA II ions (supporting information, Figure S3). We then performed CIU experiments of CA II with and without fragments. 5V increments were employed until the onset of an increase in drift time was observed; following this the increment size was reduced to 2 V to record all conformers of the protein ion during unfolding. Our first titration was conducted with apo CA II. Upon increasing activation, dissociation of the bound acetate ion was observed in the MS data and the ion was totally dissociated at a trap voltage of 30 V. Visualisation of the changes in ion drift time as a function of increasing collision energy was performed by way of a cumulative data heat map, produced using CIU Suite.[16] This revealed that at relatively low trap voltages, the drift time of CA II remained consistent (9 ms), suggesting that it adopts a compact (C) conformation under these conditions (Figure 3A). As ion activation is increased, a single unfolding event occurred between 39 and 43 V, to produce a more extended species (E conformation) of CA II with a drift time of 15 ms. This experiment was repeated in the presence of fragment **1** and by inspection of the mass spectral data as a function of increasing collision voltage it is clear that increases in kinetic energy of the complex resulted in a progressive reduction in the relative abundance of the ligand bound species being observed. Both fragment **1** and the acetate ion dissociated from the protein and at a trap voltage of 30V, no acid or acetate binding was observed (Figure 4). When comparing the CIU ion mobility data between apo- and **1**-bound CA II a similar trend in gas-phase unfolding profile was observed – a single unfolding event at an elevated collision voltage (Figure 3B). However,

by comparison of the unfolding pathway of the ligand bound form with apo-CA it was clear that, in the presence of fragment **1,** the onset of the unfolding transition occurred at a slightly higher voltage, and the unfolding transition takes place over a wider voltage range. Indeed, the presence of the C-conformation was still detected at 70V. This phenomenon was observed when analysing both the 10+ and 9+ charge states. These observations suggest that binding fragment **1** increases the stability of the compact protein conformation in the gas phase. This is clearly demonstrated by inspection of the subtraction plots between the CIU data of the apo- and **1**-bound protein using CIUSuite_compare (Figure 3C) which calculates a root-mean-square deviation (RMSD) between the two datasets of 10.45. A similar observation was observed when analysing the CIU profile of fragment **2** bound to CA, where the protein remained in its compact conformation at increased trap voltages (Figure 5A) although the effect was less pronounced than that observed for acid **1** (Figure 5B, difference plot, RMSD = 7.50).

We were conscious that this stabilising effect may have been due to the introduction of acid bound cations, resulting in potassium adducts which were present in minor amounts in our spectra (Figure 4, grey/hashtag). Ruotolo and co-workers had observed a significant stabilisation effect on collisional induced unfolding from the binding of several cations and anions.[18,19] Potassium as an acetate salt was found to have a moderate stabilisation effect, while chloride as an ammonium salt, was identified as a strongly stabilising anion. Furthermore, the combination of stabilising anions and cations as neutral salts was found to have an additive stabilisation effect.[20] To this end, we examined the effect that the addition of KCl to CA II might have on protein stability under our conditions. At a final concentration of 60 μM we were able to observe multiple potassium adducts, both with and without bound acetate. Although chloride has been reported to bind to carbonic anhydrase,[31] it did not maintain its association with the protein under our experimental conditions. As was the case in all other experiments, mass spectral data suggested that the acetate adducts were totally dissociated with collisional activation above 30 V, and the ion mobility CIU profile obtained did not suggest an increase in stability of the compact form when compared to apo CA II (Figure 5C); in fact evidence for destabilisation of the compact protein conformation was evident (Figure 5D, RMSD = 9.42). Thus, it appears that the fragment induced stabilization observed was not an artefact of inorganic salt contamination.

From inspection of these initial CIU data sets it is clear that the unfolding profile of CA II is comparatively simple, perhaps a result of the CA II folding to adopt a single domain. Therefore, the difference in the unfolding profiles of apo- and ligand-bound CA II are only apparent when the protein ions are activated at a comparatively narrow range of collision voltages –which results in the transition between the compact and extended conformation of the protein (ca 39 - 50 V; box region figure 3A). Therefore, in order to increase analytical throughput, we investigated if significant differences could be observed by monitoring ion mobility profiles at a single activation voltage. To this end, CA II in the presence of fragments **3** and **4** was investigated at a single trap voltage of 45 V. In both instances, significant portions of the C-conformation of CA II were observed. This is in comparison to the apo species which was present in only the E-conformation (Figure 6). In addition, an increase of acetate concentration

to 200 mM did not increase survival of compact conformation of the protein ion with 45 V pre-activation (Figure 6B).

4. Conclusions

To conclude, several studies have sought to understand the influence of small molecule additives in stabilising/destabilising native protein ions in the gas phase. In particular, the dissociation of inorganic anions has been shown to impart stability to a host protein even at elevated activation voltages.[18] Here, we have extended these studies by demonstrating that binding and subsequent dissociation of organic acids from CA II significantly delayed CIU in a manner which is likely analogous to inorganic anions. Importantly, even though acetate was present in high concentrations, the stabilising effect was not observed without the addition of acids **1 – 4**. Furthermore, we note that different acid fragments resulted in slightly altered stabilising effect in CIU experiments; these differences could be quantitated by calculation of the RMSD between the apo- and ligand bound CIU profiles (Figure 3) and/or the ratio of the compact to extended conformers of CA II in the arrival time distribution recorded with collisional activation at the transitional zone region (Figure 6). This suggests that the prevention of CIU by organic acids, may be tuneable to specific properties of a bound ligand, such as pKa, or charge density. Interestingly, there appears to be little correlation between fragment affinity and the stabilisation effect recorded in the IM-MS – for example, from native MS analysis **2** appears to display slightly higher affinity for CA II than **1** (Figure S1); in contrast the stabilisation of the C-conformer is more pronounced with fragment **1** binding (Figure 6). However, we do note that there seems to be correlation of between the ability of the ligand to displace acetate – indicative of binding close to the active site (fragments **1**, **2**, and to some extent **4**), and an increase in the ability to stabilise the C-conformation of CA II. These observations suggest the possibility that subtle changes to CIU profiles as a result of fragment binding may be indicative of the mode of binding; potentially opening avenues to exploit ion mobility analysis in FBDD campaigns. We stress however that the dataset used here is limited and further work using larger fragment libraries will be required to ascertain if the stabilising effect described here can be used to prioritise fragment hits arising from native mass spectrometry based FBDD screens.

5. Acknowledgements

This work was financially supported by the South African National Research Foundation (Grant Number 40410 and 116305) and the Royal Society-Newton Fund (Grant number NI160018). We thank Dr. Faye Cruickshank of the SIRCAMS mass spectrometry facility at the School of Chemistry, University of Edinburgh for technical support.

6. References

1. Lanucara F, Holman SW, Gray CJ, Eyers CE. The power of ion mobility-mass spectrometry for structural characterization and the study of conformational dynamics. *Nat Chem*. 2014;6(4):281-294. doi:10.1038/nchem.1889

2. Clarke DJ, Campopiano DJ. Desalting large protein complexes during native electrospray mass spectrometry by addition of amino acids to the working solution. *Analyst*. 2015;140(8):2679-2686. doi:10.1039/c4an02334j

3. Clarke DJ, Murray E, Hupp T, MacKay CL, Langridge-Smith PRR. Mapping a noncovalent protein-peptide interface by top-down FTICR mass spectrometry using electron capture dissociation. *J Am Soc Mass Spectrom*. 2011;22(8):1432-1440. doi:10.1007/s13361-011-0155-3

4. Loo JA. Studying noncovalent protein complexes by electrospray ionization mass spectrometry. *Mass Spectrom Rev*. 1997;16(1):1-23. doi:10.1002/(SICI)1098-2787(1997)16:1<1::AID-MAS1>3.0.CO;2-L

5. Kitova EN, El-Hawiet A, Schnier PD, Klassen JS. Reliable determinations of protein-ligand interactions by direct ESI-MS measurements. Are we there yet? *J Am Soc Mass Spectrom*. 2012;23(3):431-441. doi:10.1007/s13361-011-0311-9

6. Loo JA. Electrospray ionization mass spectrometry: A technology for studying noncovalent macromolecular complexes. *Int J Mass Spectrom*. 2000;200(1-3):175-186. doi:10.1016/S1387-3806(00)00298-0

7. Hernández H, Robinson C V. Determining the stoichiometry and interactions of macromolecular assemblies from mass spectrometry. *Nat Protoc*. 2007;2(3):715-726. doi:10.1038/nprot.2007.73

8. Hofstadler SA, Sannes-Lowery KA. Applications of ESI-MS in drug discovery: interrogation of noncovalent complexes. *Nat Rev Drug Discov*. 2006;5(7):585-595. doi:10.1038/nrd2083

9. Ben-Nissan G, Sharon M. The application of ion-mobility mass spectrometry for structure/function investigation of protein complexes. *Curr Opin Chem Biol*. 2018;42(Feb):25-33. doi:10.1016/j.cbpa.2017.10.026

10. Eyers CE, Vonderach M, Ferries S, Jeacock K, Eyers PA. Understanding protein–drug interactions using ion mobility–mass spectrometry. *Curr Opin Chem Biol*. 2018;42(Feb):167-176. doi:10.1016/j.cbpa.2017.12.013

11. Niu S, Ruotolo BT. Collisional unfolding of multiprotein complexes reveals cooperative stabilization upon ligand binding. *Protein Sci*. 2015;24(8):1272-1281. doi:10.1002/pro.2699

12. Soper-Hopper MT, Eschweiler JD, Ruotolo BT. Ion Mobility-Mass Spectrometry Reveals a Dipeptide That Acts as a Molecular Chaperone for Amyloid β. *ACS Chem Biol*. 2017;12(4):1113-1120. doi:10.1021/acschembio.7b00045

13. Stojko J, Fieulaine S, Petiot-Bécard S, et al. Ion mobility coupled to native mass spectrometry as a relevant tool to investigate extremely small ligand-induced conformational changes. *Analyst*. 2015;140(21):7234-7245. doi:10.1039/C5AN01311A

14. Young LM, Saunders JC, Mahood RA, et al. Screening and classifying small-molecule inhibitors of amyloid formation using ion mobility spectrometry-mass spectrometry. *Nat Chem*. 2015;7(1):73-81. doi:10.1038/nchem.2129

15. Cubrilovic D, Barylyuk K, Hofmann D, et al. Direct monitoring of protein-protein inhibition using nano electrospray ionization mass spectrometry. *Chem Sci*. 2014;5(7):2794-2803. doi:10.1039/c3sc53360c

16. Eschweiler JD, Rabuck-Gibbons JN, Tian Y, Ruotolo BT. CIUSuite: A Quantitative

Analysis Package for Collision Induced Unfolding Measurements of Gas-Phase Protein Ions. *Anal Chem*. 2015;87(22):11516-11522. doi:10.1021/acs.analchem.5b03292

17. Merenbloom SI, Flick TG, Daly MP, Williams ER. Effects of select anions from the Hofmeister series on the gas-phase conformations of protein ions measured with traveling-wave ion mobility spectrometry/mass spectrometry. *J Am Soc Mass Spectrom*. 2011;22(11):1978-1990. doi:10.1007/s13361-011-0238-1
18. Han L, Hyung SJ, Mayers JJS, Ruotolo BT. Bound anions differentially stabilize multiprotein complexes in the absence of bulk solvent. *J Am Chem Soc*. 2011;133(29):11358-11367. doi:10.1021/ja203527a
19. Han L, Hyung SJ, Ruotolo BT. Bound cations significantly stabilize the structure of multiprotein complexes in the gas phase. *Angew Chem Int Ed*. 2012;51(23):5692-5695. doi:10.1002/anie.201109127
20. Han L, Ruotolo BT. Traveling-wave ion mobility-mass spectrometry reveals additional mechanistic details in the stabilization of protein complex ions through tuned salt additives. *Int J Ion Mobil Spectrom*. 2013;16(1):41-50. doi:10.1007/s12127-013-0121-9
21. Doak BC, Norton RS, Scanlon MJ. The ways and means of fragment-based drug design. *Pharmacol Ther*. 2016;167(Nov):28-37. doi:10.1016/j.pharmthera.2016.07.003
22. Murray CW, Rees DC. Opportunity Knocks: Organic Chemistry for Fragment-Based Drug Discovery (FBDD). *Angew Chem Int Ed*. 2016;55(2):488-492. doi:10.1002/anie.201506783
23. Pedro L, Quinn R. Native Mass Spectrometry in Fragment-Based Drug Discovery. *Molecules*. 2016;21(8):984. doi:10.3390/molecules21080984
24. Shiu-Hin Chan D, Whitehouse AJ, Coyne AG, Abell C. Mass spectrometry for fragment screening. *Essays Biochem*. 2017;61(5):465-473. doi:10.1042/EBC20170071
25. Woods LA, Dolezal O, Ren B, Ryan JH, Peat TS, Poulsen S-A. Native State Mass Spectrometry, Surface Plasmon Resonance, and X-ray Crystallography Correlate Strongly as a Fragment Screening Combination. *J Med Chem*. 2016;59(5):2192-2204. doi:10.1021/acs.jmedchem.5b01940
26. Martin DP, Cohen SM. Nucleophile recognition as an alternative inhibition mode for benzoic acid based carbonic anhydrase inhibitors. *Chem Commun*. 2012;48(43):5259-5261. doi:10.1039/c2cc32013d
27. D'Ambrosio K, Carradori S, Monti SM, et al. Out of the active site binding pocket for carbonic anhydrase inhibitors. *Chem Commun*. 2015;51(2):302-305. doi:10.1039/c4cc07320g
28. Mazumdar PA, Kumaran D, Swaminathan S, Das AK. A novel acetate-bound complex of human carbonic anhydrase II. *Acta Cryst F*. 2008;64(3):163-166. doi:10.1107/S1744309108002078
29. Krishnamurthy VM, Kaufman GK, Urbach AR, et al. Carbonic anhydrase as a model for biophysical and physical- organic studies of proteins and protein–ligand binding. *Chem Rev*. 2008;108(3):946-1051. doi:10.1021/cr050262p.Carbonic
30. Tjernberg A, Markova N, Griffiths WJ, Hallén D. DMSO-related effects in protein characterization. *J Biomol Screen*. 2006;11(2):131-137. doi:10.1177/1087057105284218

31. Ward RL. Chlorine-35 nuclear magnetic resonance studies of a zinc metalloenzyme carbonic anhydrase. *Biochemistry*. 1969;8(5):1879-1883. doi:10.1021/bi00833a016

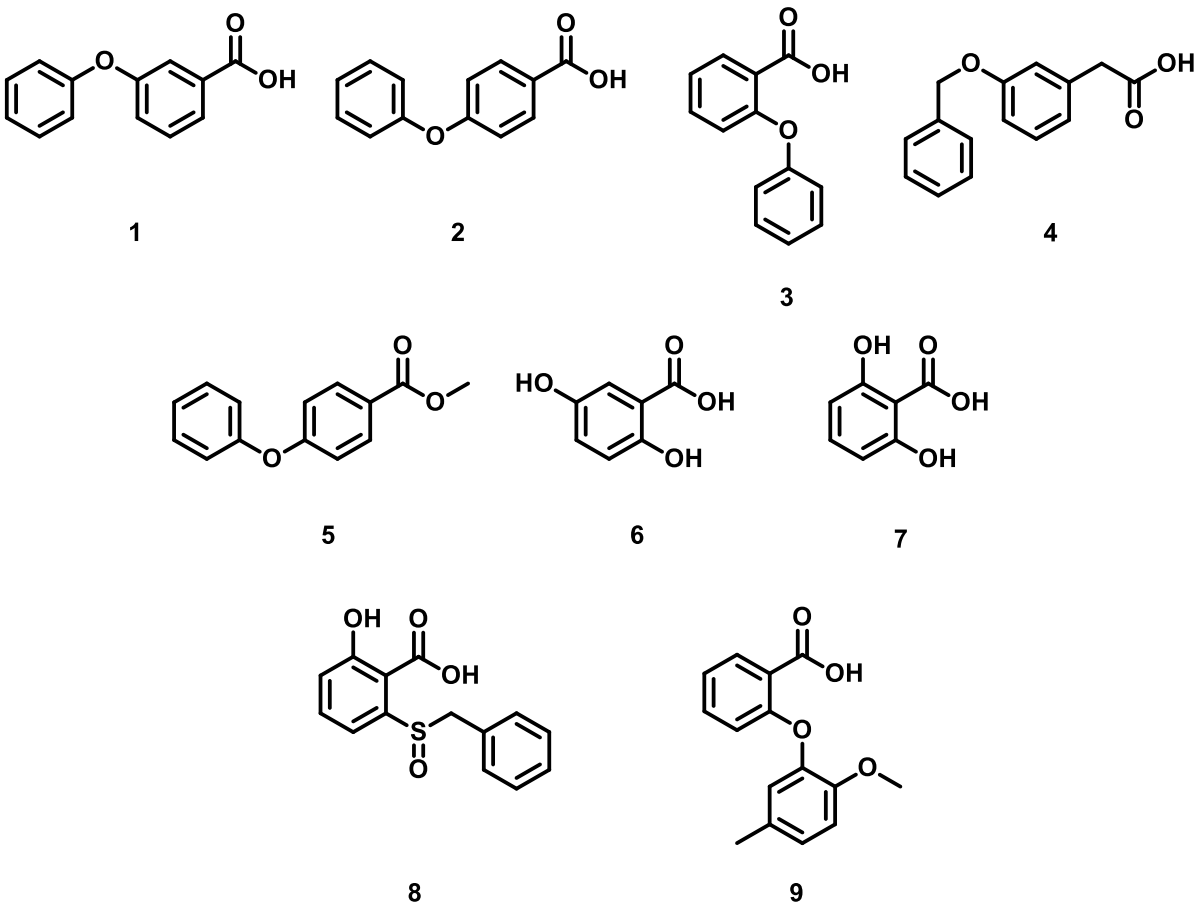

FIGURE 1. Organic acid fragments analysed for Carbonic Anhydase II binding. Fragments **1** to **5** were used in this study.

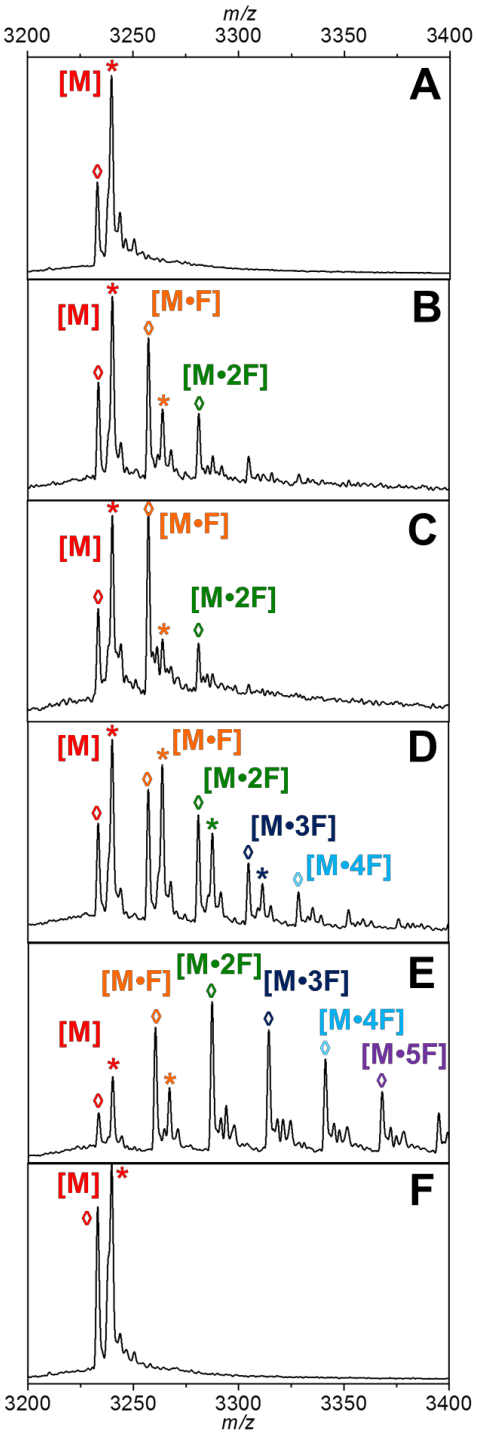

FIGURE 2. Native ESI MS analysis of CA II and fragment binding to CA II. In each case the 9+ charge state is displayed. Spectra were acquired from 10 mM NH_4OAc buffer. (**A**) apo-CA II presents without acetate bound (diamond, *m/z* 3233.2 $[M+Zn+7H]^{9+}$) and with acetate bound (asterisk *m/z* 3239.8, $[M+Zn+CH_3COOH+7H]^{9+}$). **(B) to (F)** CA II in the presence of fragment **1** (**B**) fragment **2** (**C**) fragment **3** (**D**), fragment **4** (**E**) and fragment **5** (**F**). In each spectra the number of bound ligands is indicated by color; acetate-free species are indicated with diamonds, acetate bound species are indicated with asterisk.

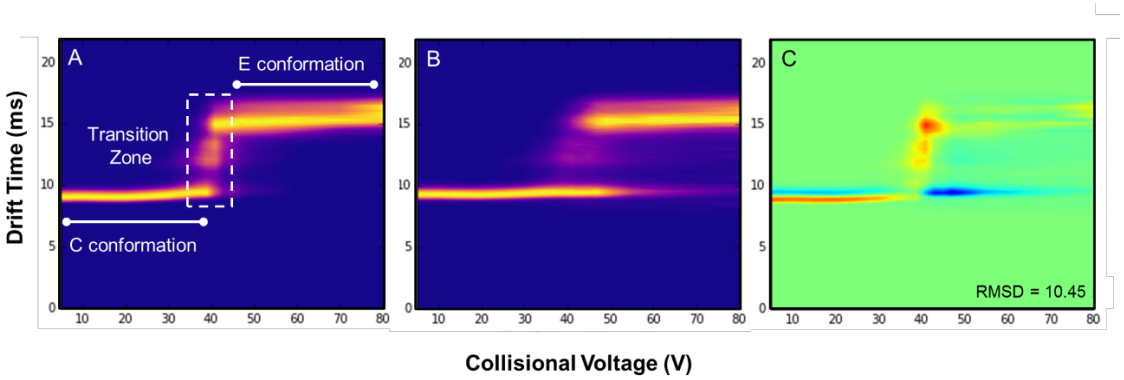

FIGURE 3. Collision Induced unfolding (CIU) of apo-CA II and fragment **1** bound CA II. Heat maps of cumulative CIU ion mobility data is shown. (**A**) apo CA II. The drift time of the 10+ apo-CA (*m/z* 2905-2920) is displayed as a function of increasing collisional energy. This map highlights the change from the compact (C-) to the extended (E-) conformation, via the transition zone. (**B**) Heat map of CA II in the presence of fragments **1**, showing the extended lifetime of conformation C. Here the drift times of all species within the 10+ charge state are considered (*m/z* 2905-2955). (**C**) Subtraction overlay of the CIU heatmaps of CAII bound to fragment **1** minus apo-CA II highlighting the RMSD between two plots.

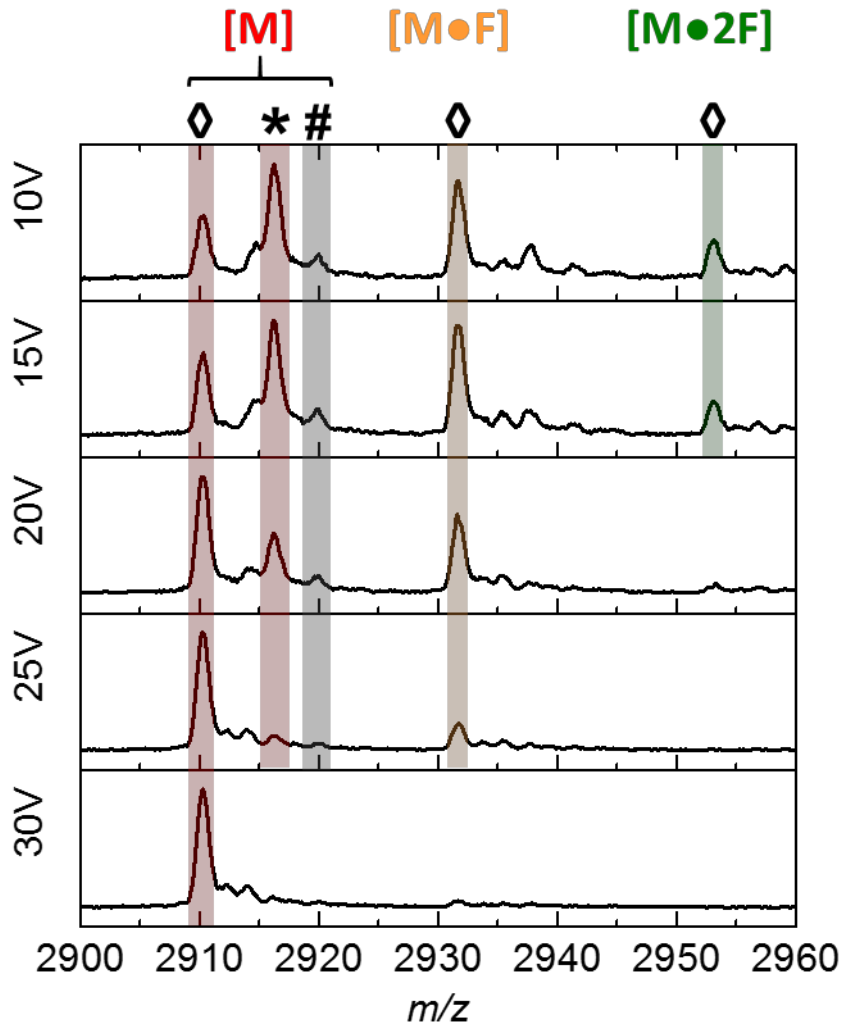

FIGURE 4. Native ESI MS of CA II bound to fragment **1** at increasing trap voltages (10 to 30 V displayed). The 10+ charge state is displayed. The species highlighted in red at *m/z* 2910.2 (diamond) and *m/z* 2916.2 (asterisk) correspond to apo CA II ($[M+Zn+8H]^{10+}$) and its acetate adduct ($[M+Zn+CH_3COOH+8H]^{10+}$) respectively. The species highlighted in orange and green correspond to the fragment bound complex with (1:1) and (1:2) stoichiometry. Increased collisional energy results in both acetate and fragment dissociation between 25 and 30 V. The minor species *m/z* 2919.9 (grey/hashtag) is consistent with a potassium adduct $[M+Zn+CH_3COOH+7H+K]^{10+}$, indicating low levels of K^+ contamination.

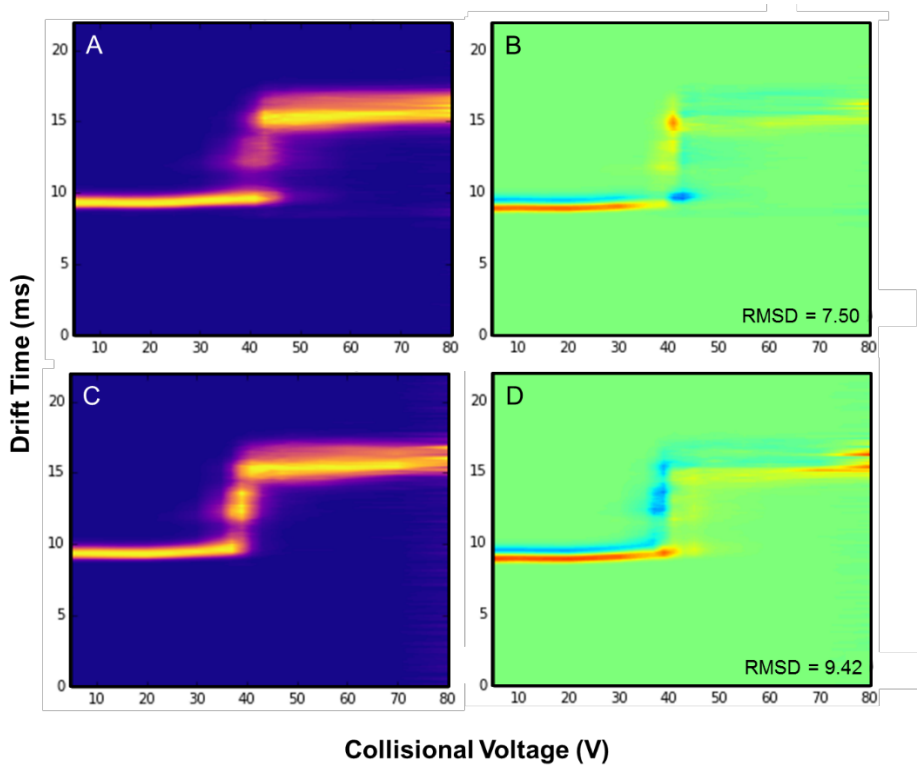

FIGURE 5. Collision Induced unfolding (CIU) of 10+ charge stae of CA II bound to fragment **2** (*m/z* 2905-2955; **A** and **B**) and KCl (*m/z* 2905-2940; **C** and **D**). ***A and C***, The unfolding curves show the transition from the C to E conformation. ***B and D***, Subtraction overlay of the CIU heatmaps of CA II bound to fragment **2** minus apo-CA II and KCl minus apo-CA II respectively.

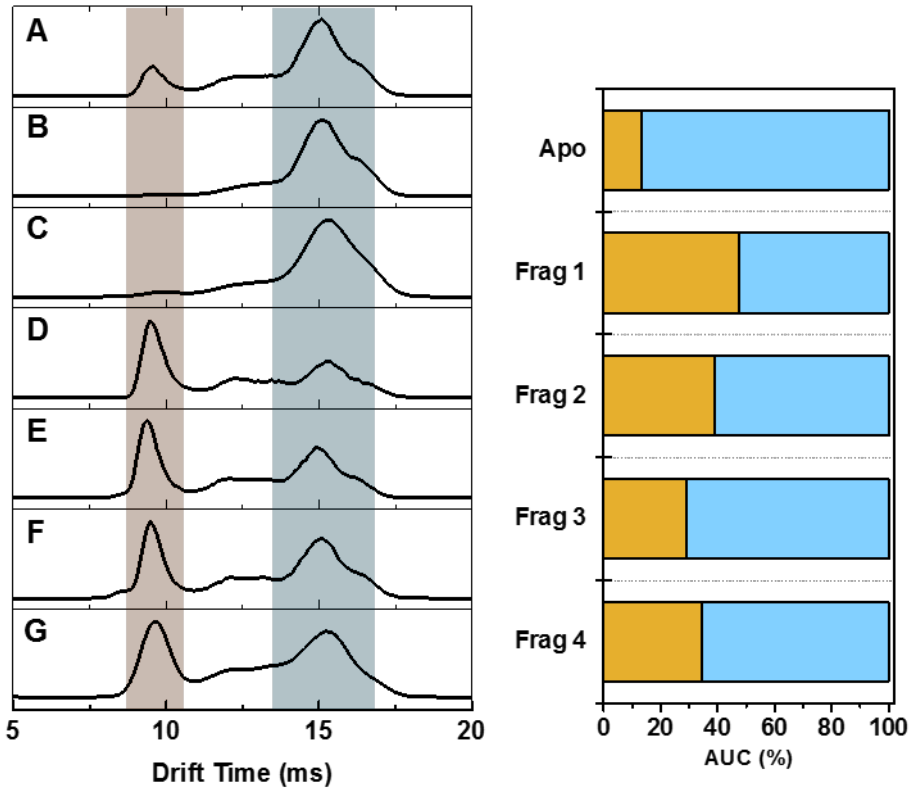

FIGURE 6. ***Left***, Comparative single point IM arrival time distributions of the 10+ charge state of CA II collected at a trap voltage of 45V. The compact (C-) and extended (E-) conformations of BA II ions are highlighted in orange and blue respectively. (**A**) Apo CA II in 10 mM NH_4OAc. (**B**) Apo-CA II in 200 mM NH_4OAc. **(C)** CA II incubated with KCl in 10 mM NH_4OAc. (**D**) – (**G**) CA II incubated with fragments **1**, **2**, **3** and **4** respectively in 10 mM NH_4OAc. **1 - 4**. ***Right***, The ratio of the C- (*orange*) and E- conformation (*blue*) determined by calculating the area under the curve of the two conformations in the arrival time distributions. This comparative analysis highlights the enhanced survival of compact conformation of CA II species at elevated trap voltages as a result of binding and dissociation organic acids.